



Key Design Trades for a Near-term Lunar Fission Surface Power System

May 2025

Changing the World's Energy Future

Lee Mason, Venkateswara Rao Dasari, Sebastian C Corbisiero



DISCLAIMER

This information was prepared as an account of work sponsored by an agency of the U.S. Government. Neither the U.S. Government nor any agency thereof, nor any of their employees, makes any warranty, expressed or implied, or assumes any legal liability or responsibility for the accuracy, completeness, or usefulness, of any information, apparatus, product, or process disclosed, or represents that its use would not infringe privately owned rights. References herein to any specific commercial product, process, or service by trade name, trade mark, manufacturer, or otherwise, does not necessarily constitute or imply its endorsement, recommendation, or favoring by the U.S. Government or any agency thereof. The views and opinions of authors expressed herein do not necessarily state or reflect those of the U.S. Government or any agency thereof.

Key Design Trades for a Near-term Lunar Fission Surface Power System

Lee Mason, Venkateswara Rao Dasari, Sebastian C Corbisiero

May 2025

**Idaho National Laboratory
Idaho Falls, Idaho 83415**

<http://www.inl.gov>

**Prepared for the
U.S. Department of Energy
Under DOE Idaho Operations Office
Contract DE-AC07-05ID14517**

Key Design Trades for a Near-term Lunar Fission Surface Power System

Lee Mason¹, Lindsay Kaldon¹, Sebastian Corbisiero² and DV Rao²

¹ NASA Glenn Research Center, Cleveland, Ohio

² Idaho National Laboratory, Idaho Falls, Idaho

Primary Author Contact Information: lee.s.mason@nasa.gov

[Leave space for Digital Object Identifier (DOI) to be added by ANS – remove this line but leave space]

NASA and DOE have been developing concepts for lunar and Mars Fission Surface Power (FSP) systems for decades and have considered many different technologies and system variations. In 2023, three contractor teams completed Phase 1 conceptual design studies on a 40 kWe lunar FSP system in response to a modest set of NASA requirements and goals. A government team consisting of NASA Glenn Research Center (GRC), Los Alamos National Laboratory (LANL), and Idaho National Laboratory (INL) was formed to develop an independent design approach that adhered to the same requirements and goals posed to the contractor teams. GRC provided expertise, analysis, and design decisions for the power conversion, heat rejection, power management & distribution (PMAD), and mission integration. LANL and INL provided expertise, analysis, and design decisions for the reactor and shielding. The goal of the government study was to develop representative concepts that could be used in NASA architecture studies, guide government technology investments, and inform Phase 2 requirements definition. This paper provides a summary of the key technology options, system-level trades, and mission-level concept-of-operations.

I. BACKGROUND

Fission Surface Power (FSP) is a Space Technology Mission Directorate (STMD) technology development project under the Technology Demonstration Mission (TDM) program. In late 2022, the FSP project awarded Phase 1 study contracts to three contractor teams: 1) Intuitive Machines & X-energy (IX), 2) Lockheed Martin & BWXT, and 3) Westinghouse & Aerojet Rocketdyne. The 1-year study contracts concluded with separate multi-day concept reviews at NASA Glenn Research Center (GRC) in Aug 2023 and delivery of the Data Product Documents (DPDs) as requested in the Statement of Work (SOW) from each contractor team in Sep 2023. The SOW provided design requirements and design goals as summarized in Table I. Each contractor team developed and evaluated a slightly different FSP design approach. IX pursued a heat pipe reactor with Stirling conversion; Lockheed, a gas-cooled reactor with Brayton conversion; and Westinghouse, a heat pipe reactor with Brayton. The

contracts are planned to continue under a Phase 1 extension (Phase 1a) where each team is performing tailored work scope based on the technical challenges posed by their individual designs. The follow-on Phase 2 contract is planned to develop a FSP demonstration system that could be delivered to the moon, and a corresponding test unit that would be extensively tested on Earth. The Phase 1 SOW requirements and goals provide a starting point for the design studies and will be revised and expanded for Phase 2 based on the initial results, the internal government studies presented in this report, and further interactions with the stakeholder community.

TABLE I. Phase 1 Design Requirements (DR) and Design Goals (DG).

DR-1	Power	40 kWe for 10 yr	DG-1	Stowed Volume	4m dia. x 6m length
DR-2	Launch & Landing Loads	7.63 g-rms launch, 4 g landing	DG-2	Total Mass	6000 kg including margin & growth
DR-3	Radiation Protection	<5 rem/yr at 1 km	DG-3	Power Cycles	Multiple on/off cycles
			DG-4	User Load	0 to 100%
			DG-5	Fault Tolerance	At least 5 kWe after fault
			DG-6	Transportability	Can be removed from lander and relocated

II. TECHNICAL APPROACH

An internal government team consisting of NASA GRC, Los Alamos National Laboratory (LANL), and Idaho National Laboratory (INL) was formed to develop an independent design approach that adheres to the same SOW requirements and goals posed to the contractor teams. GRC provided expertise, analysis, and design decisions for the power conversion, heat rejection, power management & distribution (PMAD), and mission integration. LANL and INL provided expertise, analysis, and design decisions for the reactor and shielding.

FSP system modeling was performed using GRC's *EZ FSP Sizer* which permitted sensitivity studies on key parameters and a tool to optimize the overall system with model-based reactor and shield inputs supplied by the Department of Energy (DOE) team. *EZ FSP Sizer* is a spreadsheet-based nuclear power system sizing tool developed at GRC with simple first-order calculations and hardware-based curve fits. The key design variables can be passed among the various coupled FSP subsystems to evaluate integrated system performance. The original tool was developed during the Prometheus Program to analyze the Jupiter Icy Moons Orbiter (JIMO) power plant and revised to support the Constellation-era FSP studies. It includes reactor and shield sizing algorithms that were updated based on the latest DOE provided inputs. Also included are Brayton and Stirling thermodynamic models with cycle optimization routines using iterative energy balance calculations and mass estimation based on heritage hardware and designs. A coupled heat rejection model with multiple fluids, material options, and heat transfer geometries includes the capability to assess radiator transient performance over the lunar day-night cycle. There are power conversion-tailored PMAD models with calculations to analyze the downstream power electronics, thermal management, and power transmission cabling.

The government concepts were informed by prior FSP design studies, particularly the 40 kWe FSP concept developed in 2010 by a NASA/DOE team (Ref 1) and several recent FSP mission integration studies performed by the GRC Compass team. The primary objectives of the internal government effort were: 1) acquire insights to help the government team be a smart buyer, 2) identify risks and opportunities to inform government technology investments, 3) develop concepts that can be provided to NASA architecture study teams, and 4) collect data to guide the Phase 2 Request-for-Proposal (RFP) requirements.

The activity started in 2022 with a COMPASS mission study for a transportable 40 kWe FSP system that included three separate pallets deployed from the lander (Ref 2). COMPASS had done previous mission studies that examined a 10 kWe FSP system which remained on the lander and a derivative 10 kWe version that was deployed with a single pallet. All the COMPASS studies assumed a FSP system utilizing a heat pipe reactor coupled to four Stirling converters. Beginning in Jan 2023, the FSP government team completed three Design Analysis Cycles (DACs). These explored different technology variants and alternative mission integration options of the 40 kWe system. DAC1 was completed in April 2023, DAC2 in Aug 2023, and DAC3 in Nov 2023.

III. KEY SYSTEM TRADES

Two different technology variants were pursued under the government FSP studies including a direct gas-cooled

(GC) reactor with Brayton conversion and a heat pipe (HP) reactor with Stirling conversion. Both concepts were subjected to sensitivity studies to evaluate a variety of nuclear design parameters, thermodynamic variables, waste heat rejection approaches, PMAD architectures, and shielding variants. A fundamental ground rule was adopted that both concepts utilize parallel, independent power strings for fault tolerance. Each power string includes a power conversion unit, dedicated heat rejection loop, and dedicated PMAD power channel. A failure of any component in a power string would only affect that string, allowing partial system power to be produced from the remaining strings.

GRC's FSP Parametric System Model *EZ FSP Sizer* was used to evaluate the system performance and mass sensitivities for all the design permutations evaluated in this paper. A summary of the key FSP design decisions is presented in Table II. The design decisions were made after evaluating a variety of alternative options and are consistent with the goal to deliver a FSP system to the moon in the late 2020s or early 2030s. The current Technology Readiness Level (TRL) of the FSP major subsystems is very dependent on design choices. A preliminary technology readiness assessment was performed on the selected FSP technologies, and a summary of the results is shown in Table III.

TABLE II. Key Design Decisions.

	GC-Brayton	HP-Stirling
Reactor fuel and moderator	19.75% enriched UN fuel pins, YH moderator	
Reactor heat transport method	Direct gas-cooling	Na heat pipes
Power conversion working fluid	40 mol. weight HeXe	Helium
Cycle hot-end temp	1100 K	1050 K
Cycle cold-end temp	390 K	420 K
Peak cycle pressure	1.5 MPa	7.5 MPa
Power string number and size	4 x 25%; first failure results in no less than 75% power output	
Heat rejection approach	Pumped H2O heat transport; composite radiator panels with embedded Ti/H2O heat pipes	
PMAD approach	240 Vrms alternator output, 3 kVac/1 kHz step-up, 1 km transmission, 120 Vdc load interface	
Radiation limits	<10 MRad at 1m (pwr conv), <300 kRad at 10m (controller), <5 rem/yr at 1km (crew hab)	

TABLE III. Technology Readiness Assessment.

FSP Subsystem	Current TRL
Reactor fuel element (UN, <1400K)	5
Moderator element (YH, <1100K)	4
Reactor heat pipes (Na, <1200K)	5
Radiation shield (LiH/B4C/W)	4
Reactor Inst. & Control	4
10 kWe-class Brayton power conversion (<1100K)	4
10 kWe-class Stirling power conversion (<1100K)	5
Heat rejection (400-500K)	5
PMAD (240Vac-3000Vac-120Vdc)	4

The system operating temperatures were selected after considerable deliberation and analysis. Both reactors use the same UN fuel and YH moderator technology, and the reactor operating temperatures are approximately the same. Higher reactor operating temperatures can offer performance benefits but come with greater development risk. The Stirling cycle hot-end temperature is reduced by the temperature drop caused by the heat pipe interface, while the direct gas-coupling of the Brayton with the reactor eliminates this penalty. The baseline operating temperatures in Table II are consistent with prior Brayton and Stirling converters that have been built and tested. Sensitivity studies considered a 100 K increase in hot-end temperature for both systems, corresponding to an effective 1200 K reactor supply temperature. The higher hot-end temperature analysis revealed a modest 7% system mass decrease for the GC-Brayton and a 5% decrease for the HP-Stirling, neither of which were deemed worthwhile after considering the added development risk.

The cycle cold-end temperatures were selected based on overall system mass optimization. The system mass optimization trade is presented in Figure 1 for the two candidate systems. Lower cold-end temperatures result in higher efficiency and lower reactor thermal power (smaller reactor). Higher cold-end temperatures result in increased rejection temperatures and less radiator area (smaller radiator). The Brayton design point was selected at a cold-end temperature slightly above the mass minimum (a penalty of only 70 kg) because of the sizable 15% radiator area benefit. A smaller radiator was deemed a more important feature than the modest mass savings, based on the perceived complexity of deploying large structures. At the selected cold-end temperatures, the GC-Brayton requires a 230 kWt reactor and 180 m² main radiator while the HP-Stirling requires a 175 kWt reactor and 140 m² main radiator.

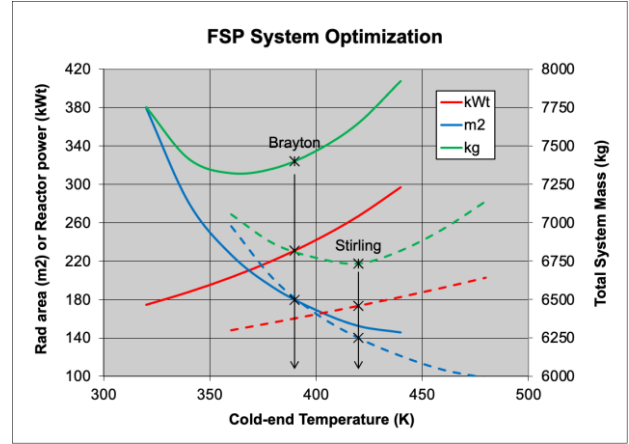


Fig. 1. FSP System Mass Optimization with Varying Cold-end Temperature (GC-Brayton option is solid curves, HP-Stirling is dashed curves)

A system-level trade that has major implications on fault tolerance (reliability) and mass is the number and size of the power strings. The baseline configuration assumes four strings at 25% power each, as shown in Figure 2. The primary options studied by the government team included two strings at 50% power, four at 50%, and two at 100%. The configurations with 100% total capacity (4x25% and 2x50%) result in a fractional decrease in system power output after a failure. The configurations with 200% total capacity (4x50% and 2x100%) can continue to produce full output power after a failure. The Brayton option benefits more by using fewer units of larger unit size due to the favorable economies-of-scale with the turbomachinery.

There is a 12% system mass decrease for the GC-Brayton in going from 4x25% strings to 2x50% strings, whereas the HP-Stirling sees only a 7% decrease. The drawback for the 2x50% configuration is that a failure of any component in the power string results in a 50% decrease in system output power. The 4x50% configuration results in a 18% mass increase for the GC-Brayton and a 30% mass increase for the HP-Stirling. The 2x100% configuration yields a 7% mass increase for Brayton and a 23% mass increase for Stirling. All these options significantly exceed the SOW goal for 5 kWe system output power after a failure. The 4x25% configuration was deemed to be the best compromise of mass, risk, and reliability. This configuration results in an FSP system that produces no less than 75% power output under any credible single failure.

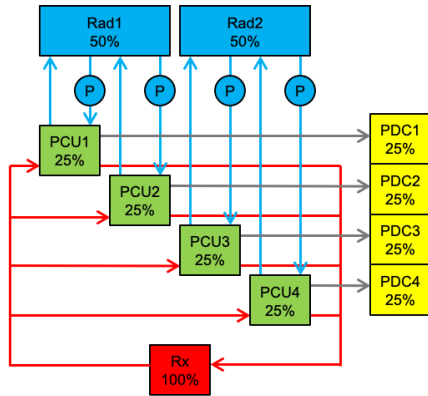


Fig. 2. Four-string FSP Configuration (Rx=reactor, PCU=power conversion unit, PDC=power distribution channel, P=pump, Rad=radiator)

IV. MAJOR SUBSYSTEMS

The FSP system consists of five major subsystems: reactor, shield, power conversion, heat rejection, and PMAD.

IV.A. Reactor

A key design decision that significantly impacts reactor mass and risk is the level of uranium fuel enrichment. Based on guidance from STMD, all design studies were to assume High Assay Low Enriched Uranium (HALEU) with U-235 isotope enriched to 19.75%. The use of HALEU typically requires the reactor designer to include a moderator in order to reduce the uranium fuel load and achieve a compact, low mass design. Candidate FSP fuel options include metallic fuel (e.g., UMo), conventional ceramic fuel (e.g., UO_2 , UN), and TRi-structural ISOtropic particle (TRISO) fuel. Candidate moderator options include metal hydrides (ZrH, YH) and beryllium compounds (Be, BeO). The LANL team analyzed multiple combinations of fuel, moderator, and reflector. UMo and TRISO fuels and Be-based moderators were excluded from further analysis due to the large size and mass of the reactor and shield. The focus of the government study was narrowed to designs that use UN fuel pins and YH moderator.

The two FSP reactor assemblies are depicted in Figure 3. Each of these reactor designs were matured to a level of fidelity and detail necessary to quantify performance, estimate mass, and assess development risk. The concepts were developed by means of computational multi-physics modeling techniques developed and benchmarked at LANL. Industry standard modeling tools such as the neutron transport code *MCNP* and the thermo-mechanical code *ABAQUS* were used to characterize reactor nuclear and thermal performance under nominal and off-design operating conditions.

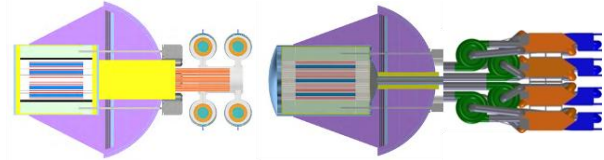


Fig. 3. FSP Reactor Assembly Concepts (HP-Stirling on the left, GC-Brayton on the right)

The 175 kWt heat pipe reactor assembly consists of a BeO monolithic core structure that is 40.5-cm in diameter and 50.2-cm in length. Pre-engineered circular channels in the monolith are used to accommodate UN fuel pins and YH moderator pins. The moderator pins are encapsulated in 0.5-cm thick titanium-zirconium-molybdenum (TZM) alloy cladding which are chemical vapor deposition (CVD) coated with tungsten to a thickness of 50-microns. The reactor core is cooled by 48 sodium heat pipes with TZM cladding providing a total capacity of 500 kWt. The thermal design allows for multiple heat pipe failures without impacting the reactor heat transport. A 1.5-cm thick multi-layer insulation (MLI) blanket is used to surround the core to minimize thermal losses and to maintain the reflector, vessel, and structural elements at suitable service temperatures below 850 K. The reactor assembly including the beryllium reflector and control drums is estimated to be 900 kg. An additional 250 kg is estimated for control drum motors, instrumentation, and miscellaneous components, resulting in a total reactor assembly mass of 1150 kg. It should be noted about 70 kg of this total is TZM alloy which is a strong neutron absorber that adversely affects the fuel loading. The use of alternative materials, such as niobium-zirconium alloys could yield some reactor mass savings.

The 230 kWt direct gas-cooled reactor includes many of the same design features as the heat pipe reactor. The higher thermal power requires a larger BeO monolith (45-cm in diameter and 57-cm long) to accommodate the UN fuel and YH moderator pins. The 40 g/mol HeXe gas working fluid has a maximum operating pressure of 1.5 MPa. A thick Haynes 230 pressure vessel is used to contain the working fluid. In-coming gas from the Brayton converters at 930 K is used for thermal management of the pressure vessel and all structural materials. The inlet gas is circulated along the vessel wall inner surface and around the reflector, control drums and various structural elements to maintain their respective thermal limits. The HeXe gas enters the reactor core at 950 K and exits at 1110 K which results in a 1100 K Brayton turbine inlet temperature. The total reactor assembly is about 1400 kg and physically larger than the heat-pipe reactor assembly. The pressure vessel and core length account for most of the mass difference. The combination of greater size and higher thermal power results in a 10% heavier shield for the gas-cooled reactor.

IV.B. Shield

The reactor radiation shield is impacted by two key design factors that affect the geometry and mass. The primary consideration is the radiation dose limit assumed at various key locations relative to the reactor radiation source, which are summarized below:

- 5 rem/yr to the habitat boundary assumed to be 1 km distance from the reactor.
- 10 MRad (Rad Si) gamma and 5×10^{14} neutron/cm² (>100 keV) to nearby components such as Stirling converters and drum motors.
- 300 kRad (Rad Si) gamma and 1×10^{12} neutron/cm² (>100 keV) to local electronic equipment including printed circuit boards.

The second factor affecting shield design is related to the choice of materials. A series of sensitivity analyses were performed to identify material combinations that resulted in the lowest shield mass. Those analyses combined with past experience and expert judgement resulted in the current government shield concepts. Tungsten major alloys (TMA) and steel are used for protection against gamma radiation. These alloys possess sufficient strength to serve both as radiation shield and structural support elements. A combination of boron-carbide (B4C) and natural lithium-hydride (LiH) are used for neutron attenuation. The LiH provides the lowest mass material for neutrons, but it has temperature limits that prevent its use near high temperature components. Therefore, B4C is used in the regions adjacent to the reactor heat pipes and gas fluid ducts, while LiH is used everywhere else. Water and lunar regolith can be very effective at dose reduction. Future analyses are planned to investigate alternate shielding strategies that include in-situ materials and lunar topography.

The current FSP shielding geometry is presented in Figure 4. Both reactors include a shaped, directional shield that is designed to limit reactor radiation to less than 5 rem/yr at the 1 km distant crew habitat boundary within a prescribed inclusion angle. The shield design also accounts for the radiation limits at the power conversion equipment and controller electronics discussed previously. The 36° included angle in Figure 4 is based on a hypothetical human outpost that is 1 km away and 1 km diameter; these values can be updated as the outpost definition matures. Note that the radiation dose in the habitat region will decrease substantially for crew and equipment located away from the 1 km boundary, and the dose will be further attenuated by natural topography, habitat structure, and crew suit materials. Preliminary analyses were performed that indicate the radiation dose outside of the included angle is around 50 rem/yr at the 1 km boundary, which would permit safe extended robotic operations or short-term crew operations.

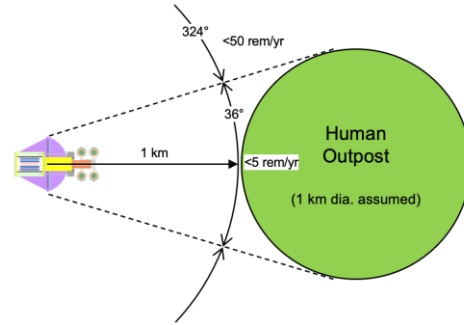


Fig. 4. FSP Shielding Geometry.

IV.C. Power Conversion

The Brayton and Stirling converter concepts are based significantly on the prior hardware prototypes as shown in Figure 5. The Brayton converter leverages the 10.5 kWe Brayton Rotating Unit (BRU) and BRU Heat Exchanger (BHXU) developed by Garrett AiResearch during the late 1960s and comprehensively tested at NASA through the mid-1970s (Ref 3). The Stirling converter leverages the 12 kWe Stirling Power Conversion Unit (PCU) developed by Sunpower for the Constellation-era FSP Technology Demonstration Unit (TDU) system test (Ref 4). The two power conversion hardware prototypes successfully demonstrated high efficiency at the specified operating temperatures using compatible construction materials and comparable heat transfer interfaces. The performance and mass models in *EZ FSP Sizer* are derived from these hardware-based references.

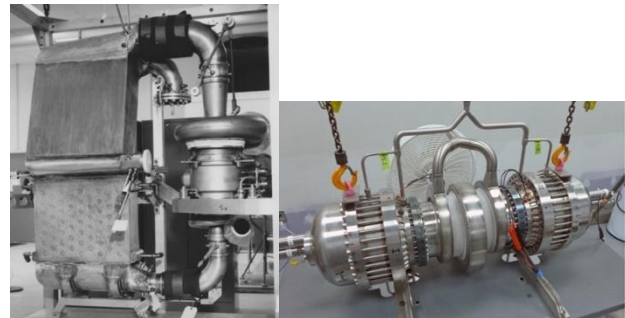


Fig. 5. Power Converter References (Brayton on the left, Stirling on the right).

The direct coupling of the GC reactor and four Brayton units results in a large, distributed gas circuit that may present challenges for working fluid gas retention over the FSP design life. A small leak would result in a gradual loss of power, while a large breach could present a single-point system failure mode. This risk is mitigated by careful material choices, judicious gas pipe routing, hermetic joints and bellows, and protective cladding and insulation to prevent micrometeoroid damage. The HP-Stirling

option includes a primary heat exchanger between the reactor heat pipes and individual Stirling heater heads. The four Stirling converters include separate working fluid pressure boundaries that preclude a single-point gas loss failure. A similar arrangement could be made for Brayton if it were coupled to a heat pipe reactor.

IV.D. Heat Rejection

Both FSP concepts use the same heat rejection technologies that were developed extensively during the Constellation-era FSP project (Ref 5). Each power conversion unit is cooled by a pumped-water heat transport loop that transfers the waste heat to a series of individual radiator panels with embedded water heat pipes. Two converters share one series-connected radiator panel assembly with a dual-pipe water manifold that couples to the evaporator section of the radiator heat pipes via a low-resistance thermal joint. The diameter of the titanium heat transport piping is optimized for minimum heat rejection mass (smaller diameter increases the pressure drop and pump power, larger diameter increases the piping mass). The radiator panel assembly is deployed vertically above the reactor and oriented in a fixed direction which results in a varying thermal sink depending on the time-of-day. The deployment approach is based on the proven scissor deployment mechanism from the International Space Station (ISS) External Active Thermal Control System (Ref 6). The water heat transport fluid (about 30-40 kg total) can be stored in a heated vessel prior to system startup to prevent freezing and could be transferred back to the vessel in the event of an extended FSP shutdown.

In order to simplify technology development and minimize manufacturing cost, a common 2 m x 2.5 m radiator panel (10 m² total surface area) is proposed. The radiator panel uses a sandwich construction with two polymer matrix composite face sheets (0.0635 cm thick, 300 W/m-K) that encapsulate fourteen Ti-H₂O heat pipes (2.5 m condenser length, 1.6 cm diameter, 14.3 cm spacing). Each heat pipe is packaged in a 2.1 cm square POCO graphite saddle, with aluminum honeycomb filler between the heat pipes for structural rigidity and launch robustness. The heat pipe spacing is optimized for minimum heat rejection mass (less spacing increases fin effectiveness to reduce radiator area, greater spacing decreases panel mass). A thermal coating is used on the radiator surface with end-of-life emissivity of 0.85 and absorptivity of 0.2. The main radiator for the HP-Stirling option must reject 119 kWt total using two radiator assemblies with 7 panels each (140 m² total) operating between 403 and 433 K. The GC-Brayton main radiator rejects 180 kWt using two radiator assemblies with 9 panels each (180 m² total) operating between 379 and 504 K. The radiator area calculations include a 10% margin. The radiator panels and heat transport loops are designed to minimize vulnerable area that might be impacted by micrometeoroid damage. Loss of an individual heat pipe

in a panel has negligible impact on radiator performance. The fractional area of heat pipes in a radiator panel is only about 10% of the radiator surface, and they are protected by the composite face sheets and graphite saddle that surrounds the heat pipe.

IV.E. PMAD

The two FSP concepts resulted in somewhat different PMAD implementations. Both use the same basic architecture consisting of a local controller and auxiliary power supply located near the reactor and a user interface located 1 km away and connected via a 3 kVac power cable. The auxiliary power supply includes a small solar array (1 kWe), rechargeable battery (4 kWh), and the required power electronics/cabling to supply FSP housekeeping power for pumps, motor drives, and instrumentation (up to 2 kWe). The DAC1 configuration assumed a separate controller pallet located 50 m from the reactor, while DAC2 and DAC3 assumed the controller and auxiliary power supply are co-located with the reactor and separated by the mechanical boom that deploys the controller radiator. An AC-based power transmission architecture was found to offer advantages over DC-based approaches for the FSP application (Ref 7). The 3 kVac, 1 kHz long-distance power transmission approach was selected to leverage the Universal Modular Interface Converter (UMIC) technology being developed by STMD (Ref 8).

The primary difference among the two PMAD implementations is the controller approach. The high-frequency 3-phase output of the Brayton alternators permit a direct coupling to the 3 kVac step-up transformer, whereas the low-frequency single-phase Stirling alternators require an additional converter stage. The resulting overall PMAD efficiency for the Brayton option is about 90% compared to 83% for Stirling. Both systems include a high-temperature (950 K) parasitic load radiator (PLR) located with the controller and sized to dissipate 120% of the total gross power. Locating the PLR near the reactor assures effective system control and permits the FSP system to demonstrate full-power production even if the remote user interface doesn't successfully deploy. Separate radiators are included at the controller and user interface to reject the waste heat from the 333 K power electronics. The Brayton option requires a 6 m² controller radiator, while Stirling requires a 18 m² controller radiator. Both systems require the same 7 m² electronics radiator at the user interface.

V. MISSION INTEGRATION

Three different mission integration options were considered as shown in Figure 6. The options generally correspond with the three Design Analysis Cycles discussed previously. Option 1 (DAC1) assumes a three pallet FSP deployment where all equipment is off-loaded from the delivery lander, similar to the concept developed

during the 40 kWe Compass study. This option results in the greatest deployment complexity, but it does permit the lander to be reused. Option 2 (DAC2) assumes that the user interface remains on the lander and the reactor pallet is deployed 1 km away. This option results in a single, large deployment of a combined reactor and controller pallet (~6t) and a lander that must be dedicated to serve as a long-term power interface node. Option 3 (DAC3) assumes that the reactor pallet remains on (or with) the lander and the user interface is deployed 1 km away. This option appears to have the simplest deployment, but it does require the lander to support long-term reactor operations. The analysis comparing the three options showed that Option 3 provided the lowest overall FSP system mass. Option 2 resulted in an FSP system that was about 10% heavier, and Option 1 was about 15% heavier.

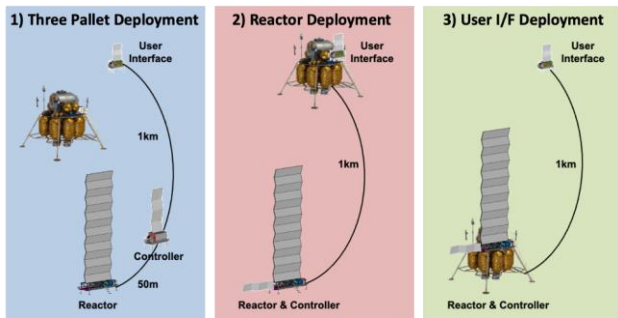


Fig. 6. FSP System Deployment Options (lander concept is notional).

The FSP system mass summary for the DAC3 configuration is presented in Table 4. The total mass includes 20% Mass Growth Allowance (MGA). Neither of the two technology options satisfy the SOW goal of 6000 kg. The HP-Stirling option provides a 10% mass savings compared to the GC-Brayton. As stated earlier, the HP-Stirling also offers the advantages of lower reactor thermal power (175 vs 230 kWt) and less main radiator area (140 vs 180 m²). The overall FSP system efficiency is 23% for the HP-Stirling option versus 17% for the GC-Brayton option. The total gross power that must be generated with the HP-Stirling option is 50.4 kWe, while the GC-Brayton generates only 46.7 kWe due to the higher PMAD efficiency. The individual converter unit power levels are 12.6 kWe for Stirling and 11.7 kWe for Brayton, which are consistent with prior hardware.

TABLE IV. FSP Mass Summary.

	GC-Brayton	HP-Stirling
Reactor Pallet (kg)	5380	4812
Reactor	1413	1132
Shield	1500	1370
Power Conversion	1182	995
Heat Rejection	884	701
Local PMAD	401	613
User Interface Pallet (kg)	872	
Main 1 km Cable & Spool	325	
Remote PMAD	273	
Command & Data Handling	72	
Structure & Installation	201	
Total FSP (kg)	6252	5683
Mass Growth Allowance (20%)	1250	1137
Total FSP with MGA (kg)	7502	6820

VI. CONCEPT OF OPERATIONS

The DAC3 approach (reactor remains with lander and user interface is deployed 1 km away) was selected to be the baseline FSP configuration pending further input from external stakeholders. During discussions with the Human-class Delivery Lander (HDL) team, they also favored this option and suggested a mission concept where the FSP could be co-manifested with a utility rover that is capable of deploying the ~1t user interface pallet. (Note: the utility rover is assumed to be a separate development and not part of the FSP project.) The two primary HDL concepts currently under study by NASA offer provisions to off-load a large payload from the lander cargo hold to the lunar surface. Conceptually, the FSP equipment and utility rover could be off-loaded from the HDL to the surface with the user interface pallet pre-loaded on the utility rover and the 1 km cable pre-connected to the reactor pallet. The utility rover would then drive the user interface pallet to its final operational site while unfurling the 1 km cable. The common 3 kVac power transmission interface at the reactor pallet results in the user interface pallet being identical for either the GC-Brayton or HP-Stirling option.

Figure 7 shows the stowed and deployed versions of the reactor pallet for the two concepts, including the main radiators and local PMAD. The stowed pallet conforms to the SOW goal of 4 m diameter and 6 m length. The main radiator for the GC-Brayton option is approximately 18 m tall after deployment, while the HP-Stirling radiator is about 14 m tall. The local PMAD electronics are located in an enclosure at the end of the 5 m controller radiator

boom and protected by the reactor’s directional shield to minimize radiation effects. Additional spot shielding can be added within the electronics enclosure if needed. Note the smaller controller radiator for Brayton due to the higher efficiency of the voltage step-up electronics.

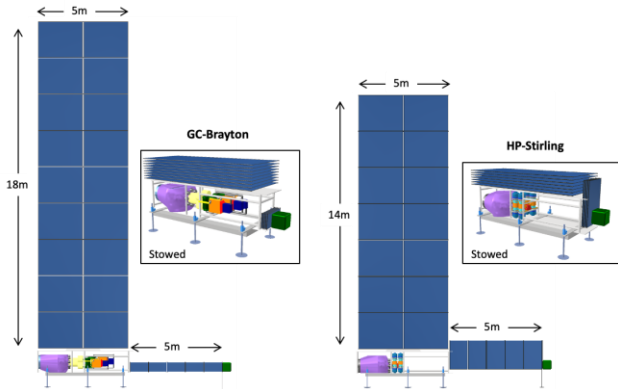


Fig. 7. FSP Reactor Pallet Layouts.

The FSP systems are designed to produce 40 kWe net output power when the lunar sink temperature is at the SOW specified value of 270 K. The actual FSP output power will vary depending on location, time-of-year, and time-of-day. The lunar equator and south pole represent bounding cases. At the south pole, the sink temperature for a fixed, vertically oriented radiator varies between 100 K and 200 K. The HP-Stirling system will produce a minimum power output of 40.7 kWe, a maximum of 41.7 kWe, and a synodic period average of 41.1 kWe. At the lunar equator, the sink temperature for the vertical radiator varies between 100 K and 320 K. There, the HP-Stirling system produces a minimum of 38.6 kWe, a maximum of 41.7 kWe, and an average of 40.5 kWe. The GC-Brayton option will perform similarly, but with slightly different values for minimum, maximum, and average power.

The 1 km main power cable is actually four separate 3 kVac power feeds (10 kWe each, 3x14 AWG wires) to preserve the channel redundancy provided by the four-string architecture. Each power channel includes an additional fiber-optic communication wire for FSP data transmission. The main cable is housed on a common spool with four separate reels to permit some physical separation between the feeds as they are deployed on the surface to reduce the potential for cross channel failure modes. The cable’s location on the lunar surface affords a 180° view to space for heat rejection; burying the cable is not advised due to the poor thermal conductivity of the regolith. The main power feeds could be bidirectional, permitting an external power source to supply startup power to the FSP reactor from the user interface if the reactor pallet’s on-board auxiliary power supply is unable to perform.

The user interface pallet developed for the Compass study and shown in Figure 8 is representative of what would be needed for the DAC3 system. The stowed pallet which must be deployed by the utility rover is approximately 2.8 m long by 1.6 m wide by 1.2 m tall. The DAC3 version includes the Command and Data Handling (C&DH) equipment to receive FSP commands and transmit performance data using an assumed local lunar communications network (separate development from FSP). FSP operations will be mostly autonomous with a modest number of commands for startup, shutdown, and desired fraction-of-full power. Health monitoring data rates will be typical of other lunar surface assets and not present any special technology challenges. The long-distance data wires and remote C&DH interface assures a reliable data stream that won’t be adversely impacted by the reactor radiation. The details of how the FSP user interface communicates with the local network and between Earth ground stations will be further defined as the overall lunar mission evolves.

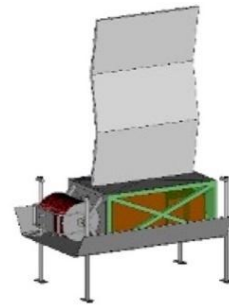


Fig 8. Representative User Interface Pallet.

VI.A. System Startup

Both systems would undergo a very similar installation and startup procedure. The reactor pallet is off-loaded from the delivery lander and placed nearby on the lunar surface while the user interface pallet is driven away. The automated startup sequence would be performed with an Earth command transmitted via the user interface pallet, which could remain near the reactor during the startup if desired. The first step is to verify reactor operation by turning the control drums to initiate the fission reaction at a very low thermal output power. After a suitable reactor temperature increase is detected, the water heat rejection loops will be filled, and the water pumps started while maintaining the radiator panels in their stowed configuration. Reactor thermal power will be gradually increased until a suitable power conversion starting temperature is achieved. One of the four converters will be started and stable operation at low electric power output will be verified before starting subsequent converters. The system parasitic loads (pumps, control drive motors, etc.) can now be switched to draw power from the FSP system rather than the on-board battery.

After all four converters are stable and operating at low power, sufficient waste heat will be present to allow the main radiator and controller radiator to be deployed without the risk of freezing. (Designing the radiators so that they can be restowed may be desirable for extended FSP shutdown periods or if the system must be relocated.) After the radiators are deployed, the reactor control drums can be adjusted to produce full power and temperature. All the electric power produced by the converters will be dissipated by the on-board PLR, until a command is sent to transmit power to the remote user interface. During operation, the PLR dissipates any excess power that is not required by the user loads. The entire startup sequence could be completed in less than 8 hours with all the startup power supplied by the on-board battery and solar array. If the user interface remained near the reactor for startup, it would be moved to its final operational site after the system achieves a stable operating condition.

The FSP user interface pallet effectively becomes a power node from which all interested users can connect via their own supplied 120 Vdc power cable. Its location would be determined based on the goal of serving the maximum number of users. Conceptually, the FSP user interface could be the first node of an extendable lunar power grid. The FSP user interface would include multiple power ports for users to share the electric power supplied by the FSP reactor pallet. Since the user interface is at a safe separation distance from the reactor, it can be accessed by crew members (or robots) for cable connections and maintenance, as needed. The reactor pallet could also be serviced, but it would require a temporary shutdown and an extended radiation cool-down period (probably months) to permit short-term crew access. At the present, there are no plans for reactor pallet maintenance during its 10-year design life.

If desired, the user interface pallet could also be moved to another location to maximize its utility. Such an operation would require the FSP main power feed to be temporarily disabled (and probably disconnected). The FSP system could continue to operate with all the power dissipated by the PLR. The new location would be constrained to remain within the 36° shield angle at a distance no greater than the 1 km length of the main power cable. Another possibility is a high voltage cable extension that could be added to the original 1 km cable to allow the user interface to be placed at further locations. The detailed Con-Ops associated with FSP power connections and maintenance can be determined after the lunar surface mission is better defined. At this time, the features discussed here are hypothetical and are not currently part of the FSP requirements set.

VII. SOME WHAT-IFS

There are several key FSP design parameters that remain uncertain and are subject to change as the lunar

mission is further defined. The current 40 kWe FSP power level may be too large for early Artemis missions and too small for future commercial lunar missions. A 40 kWe FSP might be suitable for a mission concept where all the current Artemis elements (e.g., Lunar Terrain Vehicle, Pressurized Rover, Multi-Purpose Hab) depend on a centralized power source with a grid that permits power sharing. This architecture makes sense for a permanent, fixed base that is revisited and expanded over time. An alternative Artemis mission approach is to visit multiple lunar sites with fewer surface elements that can be more easily landed and/or relocated. In this case, a smaller FSP in the 10-20 kWe class may be a better choice. A derivative 10 kWe FSP system would weigh 3.4t for the GC-Brayton option and 2.5t for the HP-Stirling option (including 20% MGA). A 20 kWe version would weigh 4.6t and 4.0t, respectively for the GC-Brayton and HP-Stirling.

At the other end of the spectrum are large commercial missions with industrial scale mining and propellant production. In this case, a larger FSP in the 80-100 kWe class may be needed. A derivative 80 kWe FSP system would weigh about 10.8t for the GC-Brayton option and 10.7t for the HP-Stirling. The 100 kWe version would weigh about 12.3t and 12.5t, respectively for the GC-Brayton and HP-Stirling. Table 5 summarizes the system performance for the five power levels that were analyzed during DAC3. The mass differences among the two options are relatively small, especially at the higher power levels. The cross-over point when the GC-Brayton system has lower mass than the HP-Stirling systems occurs around 90 kWe.

TABLE V. FSP System Comparison for Variable Power Output (mass includes 20% MGA).

FSP System Power	10 kWe	20 kWe	40 kWe	80 kWe	100 kWe
GC-Brayton System Mass (t)	3.4	4.6	7.4	11.0	12.5
Reactor Thermal Power (kWt)	72	120	230	421	517
Main Radiator Area (m ²)	57	93	180	317	380
HP-Stirling System Mass (t)	2.7	4.1	6.8	10.7	12.6
Reactor Thermal Power (kWt)	49	90	175	343	429
Main Radiator Area (m ²)	40	80	140	279	351

There are other factors to consider in choosing an FSP power level. Larger FSP systems will increase the complexity of earth-based ground testing due to the larger facilities and ground support equipment that will be needed. A larger FSP system will also be more difficult to process during pre-launch ground transportation and during the Assembly, Test and Launch Operations (ATLO) phase at the launch site. Further, the larger FSP will present greater challenges for stowing the system on the

lander, off-loading the equipment from the lander, deploying the radiators, and moving the user interface pallet into position.

The FSP power level decision should consider the various tradeoffs between having one large system versus multiple smaller systems. Meeting a specified power requirement with a single large system offers mass advantages, while multiple smaller systems offer reliability benefits due to the redundancy provided. Multiple smaller systems could also provide advantages by allowing them to be co-located with specific users. For example, separate 10 kWe FSP systems could be allocated to hypothetical users such as the crew habitat, crew ascent stage, ISRU mining equipment recharge station, and oxygen production plant. These FSP systems could also be temporarily shut down, moved, and re-allocated for other uses as needs arise. If a single 40 kWe FSP were used in the scenario above, it would require an extended power grid to permit power sharing among the four users and would likely be too large to relocate. Assuming the HP-Stirling option, the four 10 kWe systems would have a total mass of 10t while the single 40 kWe unit would weigh 6.8t plus the mass of the power grid. The use of two 20 kWe systems would weigh 8t, a mass increase of less than 17% compared to the 40 kWe system. Figure 9 shows the mass differences of using multiple HP-Stirling systems compared to a larger single system for a variety of power levels. The GC-Brayton would exhibit similar trends, but with greater mass penalties for using multiple smaller systems over a single large system.

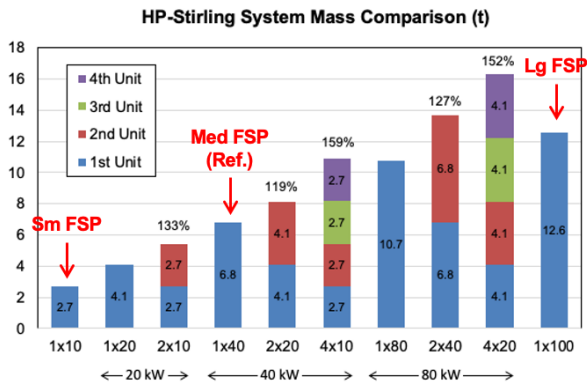


Fig 9. Mass Comparison for Single vs Multiple HP-Stirling Systems.

Another parameter that could change as the mission evolves is the FSP separation distance and cable length. Figure 10 presents the mass sensitivity as separation distance is varied. Shorter distances result in a heavier radiation shield while longer distances result in a heavier power transmission cable. The reference 1 km separation distance yields a user interface pallet that weighs 872 kg and a reactor shield that weighs 1370 kg for the HP-Stirling

option. If the cable length were reduced in half to 0.5 km, the user interface pallet mass would decrease to about 670 kg. However, the reduced separation distance would increase the shield mass to approximately 2700 kg, a net system mass increase of 1100 kg. A major portion of the shield mass increase is attributed to the larger 52 deg included angle for the new shield geometry (0.5 km separation, same 1 km outpost diameter). If the cable length were doubled to 2 km, the user interface pallet mass would increase to 1250 kg and the shield mass would decrease to about 700 kg for a net system mass decrease of about 300 kg. Here, the shield mass benefits by the smaller 22 deg included angle at 2 km. While the larger separation distance offers a modest overall system mass benefit, the risk of deploying the longer cable may negate the benefit. Figure 10 indicates that a minimum system mass occurs at a separation distance of about 1.8 km, although the total mass does not vary much between 1 and 2.5 km. A more important factor may be the mass and size of the user interface pallet, which may be limited by the utility rover that must move it.

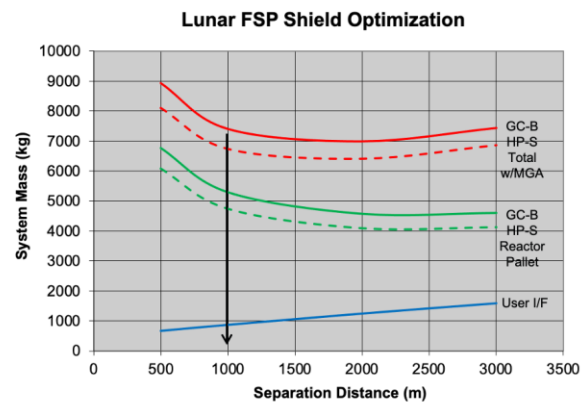


Fig 10. FSP Mass Trends with Varying Separation Distance (GC-Brayton option is solid curves, HP-Stirling is dashed curves, User I/F is same for both).

Analysis was also performed to assess the user interface pallet mass sensitivities to transmission voltage. Reducing the transmission voltage from 3 kVac to 1 kVac resulted in a 1442 kg user interface pallet, an increase of 570 kg. There was no mass benefit to increasing the voltage above 3 kVac since higher voltages resulted in wire sizes below the minimum deemed practical for this application. If the transmission distance was appreciably larger than the 1 km baseline, transmission voltages greater than 3 kVac might be considered.

VIII. CONCLUSIONS

The FSP project is evaluating design concepts by an internal NASA-DOE study team in parallel with three contractor teams that are responding to the same system requirements and goals. The 40 kWe FSP concept

developed by the government team weighs about 7t (including MGA) based on a configuration where the reactor pallet remains with the delivery lander and the user interface pallet is deployed 1 km away. The HP-Stirling approach offers a 10% mass advantage over the GC-Brayton option. The HP-Stirling system also provides the benefit of lower reactor thermal power and reduced radiator area. The GC-Brayton system simplifies the PMAD architecture, which is manifested in higher PMAD efficiency and lower gross power generated for the same net power delivered. Trade studies were performed to assess FSP system performance for a variety of configurations and design parameters. A notional concept-of-operations was developed for a baseline configuration which provides a starting point for future, more-detailed studies. Several “what if” analyses were performed to assess the system mass sensitivity for different power levels and cable lengths.

REFERENCES

1. Fission Surface Power System Initial Concept Definition, [NASA/TM-2010-216772](#).
2. A Deployable 40 kWe Lunar Fission Surface Power Concept, [NETS 2022](#).
3. Design and Fabrication of the Brayton Rotating Unit, [NASA CR-1870](#).
4. Free-Piston Stirling Power Conversion Unit for Fission Power System, Phase II Final Report, [NASA/CR-2016-219088](#).
5. Heat Pipes and Heat Rejection Component Testing at NASA Glenn Research Center, [NASA/TM-2012-217205](#).
6. International Space Station, Active Thermal Control System (ATCS) Overview, [NASA link](#).
7. Lunar Power Transmission for Fission Surface Power, [NETS 2022](#).
8. A Modular AC to DC Interface Converter to Enable Lunar Surface Power Transmission, [ASCEND 2023](#).